Electrical Resistivity of Alkali-Lead Binary Alloys

T. Khajil[ab]

[a] Department of Physics, University of Jordan, Amman, Jordan [b] Teacher's College of Education Salalah, Salalah, Sultanate of Oman

PLEASE SCROLL DOWN FOR ARTICLE

ELECTRICAL RESISTIVITY
OF ALKALI-LEAD BINARY ALLOYS

T. KHAJIL*

Department of Physics, University of Jordan, Amman, Jordan

The electrical resistivity of liquid Li–Pb, Pb–K and Pb–Na binary alloys as a function of compassion has been calculated using Faber-Ziman formalism modified for finite mean free-path. The partial structure factors described by hard sphere model of Ashcroft and Langreth are used in the calculations. The nonlocal pseudopotentials of Heine-Abarenkov have been used also. The calculated resistivity values are in reasonably good agreement with the experiment.

1. INTRODUCTION

Electrical resistivity measurements on liquid Li–Pb, Pb–K and Pb–Na alloys exhibit a sharp peak at $c_{Pb} = 21$ at% for Li–Pb, at $c_{Pb} = 49$ at% for Pb–K and at $c_{Pb} = 20$ at% for Na–Pb [1, 2]. The temperature derivative of resistivity $d\rho/dT$ is extremely large and negative at the same compositions [3]. Van der marel *et al.*, have attributed these effects to strong chemical interactions between the components. It is argued that the interactions tend to reduce the density of states at fermi level.

The widely used Faber-Ziman (FZ) theory [4] for electron transport which is based on the relaxation time approximation for Boltzman equation, needs modification when applied to finite-mean-free path l

*Address for correspondence: Teacher's College of Education Salalah, Salalah, P.O. Box 1905, Sultanate of Oman.

systems. This is because the Faber-Ziman formalism utilizes a perfectly sharp fermi surface. The finite mean free path corresponds to a finite uncertainty in the electron position. This in turn means a finite uncertainty in the electron momentum. Therefore, the Fermi surface is not perfectly sharp, but it is blurred. March and collaborators [5, 6] have taken this blurring into account by starting with the resistivity given in terms of the force–force correlation function. This treatment gives an integral equation for l-based mainly on second order perturbation theory. We have used this approach for a number of finite-l liquid metals and alloys [7, 8].

A self-consistent approach to the resistivity problem given by Ferraz and March was subsequently extended by Leavens et al. [6] and has been used successfully by Ascough and March (AM) [9] for expanded fluid rubidium. One of the most important improvements of this approach was the use of an non-local first-principles scattering potential.

In this work a further application of the scheme outlined by AM is used to calculate the resistivity of the above mentioned alloys and compared to the FZ results. In the first approach a non-local Heine-Abarenkov pseudopotentials screened through a dielectric function that includes the influence of mean free path is used.

2. THEORY

2.1. Resistivity

The resistivity for liquid metal binary alloys given by FZ can be written as

$$\rho_{FZ} = \frac{3\pi m^2}{4e^2\hbar^3 n k_f^6} \int_0^\infty dq \, q^3 \lambda(q)\theta(2k_f - q) \tag{1}$$

where

$$\lambda(q) = v_1^2(1-c)S_{11} + 2\sqrt{c(1-c)}v_1 v_2 S_{12} + cv_2^2 S_{22} \tag{2}$$

$V_i(q)$ denotes to electron-ion pseudopotentials while $S_{ij}(q)$ is the partial structure factors. In all equations, c is used as the concentration

of the second species and n is the conduction electron density related to Fermi wave number k_f by:

$$k_f = (3\pi^2 n)^{1/3}$$

In Eq. (1), θ is the unit step function that cuts off the q-integration at $(2k_f)$ corresponding to a perfectly sharp Fermi surface. The finite mean-free-path corresponds to a finite uncertainty in the electron position. This is turn corresponds to a finite uncertainty in electron momentum. Thus, the Fermi surface is not perfectly sharp but its blurred. An attempt to take this blurring into account in the formulation of resistivity is given by Ferraz and March. Starting from the force–force correlation function formula for resistivity, they replaced Eq. (1) by

$$\rho_{FZ} = \frac{3\pi m^2}{4e^2 \hbar^3 n k_f^6} \int_0^\infty dq\, q^3 \lambda(q) \Gamma(q, k_f, \ell) \tag{3}$$

$$\Gamma(q, k_f, \ell) = \frac{2}{\pi}\left[\arctan(q\ell) - \frac{1}{2}\arctan\left(\frac{2q\ell}{1 + 4k_f^2\ell^2 - q^2\ell^2}\right)\right.$$
$$\left. - \frac{\pi}{2}\theta\left(q - \left(\frac{1}{\ell^2} + 4k_f^2\right)^{\frac{1}{2}}\right)\right] \tag{4}$$

The above expression is obtained by borrowing an argument for simplification of the energy derivative of the Dirac density matrix σ evaluated at Fermi energy. The mean free path l can be determined self-consistency by calculating ρ_{FM} for $l \to \infty$ and then by using Drude relation

$$\rho = \frac{\hbar k_f}{ne^2\ell} \tag{5}$$

To find l, then Eq. (3) and Eq. (5) are iterated to self-consistency.

Ascough and March improved the work of Ferraz and March by including the influence of l on the bare-electron-ion pseudopotentials through the dielectric function of the perturbed electron gas. Ferraz and March give:

$$\sigma(k) = \frac{4m\ell n}{\pi\hbar^2 k}\left[\frac{1}{1 + 4\ell^2(k - k_f)^2} - \frac{1}{1 + 4\ell^2(k + k_f)^2}\right] \tag{6}$$

Defining the function

$$\theta(q) = \frac{\hbar^4 q}{8\pi m^2 n^2} \int \sigma(\vec{k})\sigma(\vec{k}+\vec{q})d\vec{k} \qquad (7)$$

and

$$|V_{\text{eff}}^{\ell}(q)|^2 = \frac{\int |V(\vec{k},\vec{k}')|^2 \sigma(\vec{k})\sigma(\vec{k}')d\vec{k}'}{\int \sigma(\vec{k})\sigma(\vec{k}')d\vec{k}'}, \qquad (8)$$

where $V(\vec{k},\vec{k}')$, is the non-local screened electron-ion interaction and $\vec{q} = \vec{k}' - \vec{k}$, so that the mean free path is found to be

$$\frac{1}{\ell} = \frac{3\pi m^2}{2\hbar^4 k_f^5} \int_0^{\infty} q\lambda(q,\ell)\theta_\ell(q)dq \qquad (9)$$

where

$$\lambda(q,\ell) = |V_{\text{eff},1}^{\ell}(q)|^2(1-c)S_{11} + 2(c(1-c))^{\frac{1}{2}}|V_{\text{eff},1}^{\ell}(q)||V_{\text{eff},2}^{\ell}(q)|S_{12}$$
$$+ c|V_{\text{eff},2}^{\ell}(q)|^2 S_{22} \qquad (10)$$

The dielectric function will take into account influence of the mean free path l using:

$$\varepsilon(q,\ell) = 1 - (1-G(q))\frac{4\pi e^2}{q^2}f(q,\ell) \qquad (11)$$

where

$$f(q,\ell) = -\frac{mk_f}{2\pi^2\hbar^2}\left\{1 - \frac{1}{2k_f\ell}\left(\tan^{-1}\left[\frac{4k_f\ell}{1+(q\ell)^2-(2k_f\ell)^2}\right]\right.\right.$$
$$\left. + \pi\theta(4k_f^2 - q^2 - \ell^{-2})\right) + \frac{1 - (\frac{q}{2k_f})^2 + (\frac{1}{2k_f\ell})^2}{8(\frac{q}{2k_f})}$$
$$\left. \times \ln\left[\frac{((q\ell)^2 + 1 + 2k_f\ell q)^2 + (2k_f\ell)^2}{((q\ell)^2 + 1 - 2k_f\ell q)^2 + (2k_f\ell)^2}\right]\right\} \qquad (12)$$

The local field term $G(q)$ is independent of l, and the form of this function used was due to Ichimaru and Utsumi [10]. Finally the

resistivity formula takes the form

$$\rho_{AM} = \frac{3\pi m^2}{4e^2\hbar^3 nk_f^6} \int_0^\infty dq\, q^3 \lambda(q, \ell_0)\theta_{\ell_0}(q) \tag{13}$$

where ℓ_0 is the mean free path value and is to be determined self-consistently from Eqs. (7), (8) and (9). The resistivity is calculated using Eq. (13), and in this case $\theta_{\ell_0} \to \Gamma$ evaluated at $\ell = \ell_0$.

2.2. Pseudopotentials

The pseudopotentials used in these calculations are a non-local Heine-Abarenkov model potential [11 – 15].

$$V(k, k') = \frac{V(q)}{\varepsilon(q)} + f(q, k, k') + g(q) \tag{14}$$

where $V(q)$ is the local part of the unscreened potential and is given by

$$V(q) = -\frac{8\pi A_2}{\Omega q^2}\left[\sin(qR_m - qR_m)\cos(qR_m)\right] - \frac{8\pi Z}{\Omega q^2}\cos(qR_m). \tag{15}$$

Also

$$f(q, k) = -\frac{8\pi R_m^3}{\Omega}(A_0 - A_2)\left[J_0^2(kR_m) - \frac{1}{kR_m}\cos(kR_m)J_1(kR_m)\right]$$
$$- \frac{12\pi R_m^3}{\Omega}(A_1 - A_2)\left(1 - \frac{q^2}{2k^2}\right)[J_1^2(kR_m) - J_0(kR_m)J_2(kR_m)] \tag{16}$$

For $k = k'$ and for $k = k'$

$$f(q, k, k') = -\frac{8\pi R_m^2(A_0 - A_2)}{\Omega(k^2 - k'^2)}[kJ_1(kR_m)J_0(k'R_m) - k'J_1(k'R_m)J_0(kR_m)]$$
$$- \frac{24\pi R_m^2(A_1 - A_2)}{\Omega(k^2 - k'^2)}\frac{(k^2 + k'^2 - q^2)}{2kk'}$$
$$\times [kJ_2(kR_m)J_1(k'R_m) - k'J_2(k'R_m)J_1(kR_m)] \tag{17}$$

Finally $g(q)$ in Eq. (14) is defined by

$$g(q) = \frac{8}{\pi^2 q^2 \varepsilon(q)} \int_0^{k_f} \frac{d^3\vec{k} f(k,q)}{k^2 - |\vec{k} + \vec{q}|^2} \qquad (18)$$

2.3. Structure Factors

Our calculations were carried out with Ashcroft-Langreth hard sphere partial structure factors [15], the hard sphere diameters being obtained from pure metallic data as a function of temperature. The experimental densities of pure metals used here are taken from Waseda [16]. The packing fractions are calculated using the empirical law given by Waseda and kept constant throughout the concentration range.

$$\eta_i = A_i e^{-B_i T} \qquad (19)$$

The parameters A_i and B_i appearing in this equation are taken from [16] also. The hard sphere diameters are calculated using

$$\sigma_i^3 = \frac{6\eta_i \Omega^*}{\pi} \qquad (20)$$

where Ω^* is the mean atomic volume in the alloy case and is related to the Fermi wave vector by

$$k_f^3 = \frac{3\pi^2 Z^*}{\Omega^*} \qquad (21)$$

Here Z^* is the mean valence. Both Ω^* and Z^* were obtained by a linear interpolation of the pure metal values.

3. RESULTS AND CONCLUSIONS

Following the theoretical schemes outlined above, the effects of mean free path corrections to the Faber-Ziman resistivity formula were computed for Li−Pb, Na−Pb and K−Pb liquid binary alloys, using Ashcroft-Langreth model structure factors and non-local Heine-Abarenkov model potentials. For each step, a self-consistent mean

free path was determined iteratively, using Eqs. (6)–(9) and when satisfactory convergence was obtained the corresponding resistivity was calculated.

The input parameters for pseudopotentials and structure factors are given in Table I. The hard sphere diameters were calculated using Eq. (20) and the constants A, B were taken from Ref. [16].

The calculated structure factors, as a representative case, for Pb–Na are shown in Figure 1.

Figures 2a and 2b show the calculated local and non-local pseudopotentials for Pb and Na at $c = 0.8$ separately. From these figures we notice that the peak of the non-local potentials is greater than the local one and this affects the calculated resistivity values. The coworkers of Gasser [17–19] have discussed the effect of nonlocality on the calculation of resistivity extensively, for example.

Using the same input parameters the resistivity has been calculated by two methods, one using (FZ) formula with local potentials and the other using the (AM) formalism with nonlocal potentials. The calculated resistivity values as a function of concentration for Pb–Na, Pb–K and Pb–Li are shown in Figures 3, 4 and 5 respectively along with the experimental values taken from Ref. [1]. The agreement between theoretical and experimental values are satisfactory for all alloys. The calculated peak value using the AM approach is slightly overestimated for all alloys while they are under estimated using (FZ). As discussed by Van Der Lugt *et al.* [1, 2] the alkali–lead alloys exhibit a compound forming character at A_4B and this character has been shown using the (AM) method where the mean free path effect has the main role in these results. Generally there is some shift of the peak position and this expected since the model structure factor used in these calculations need to be modified especially for these kinds of alloys.

TABLE I   Input parameters for Li–Pb, Pb–K and Pb–Na liquid metal alloys. Structural data are in atomic units and potential parameters are in rydbergs

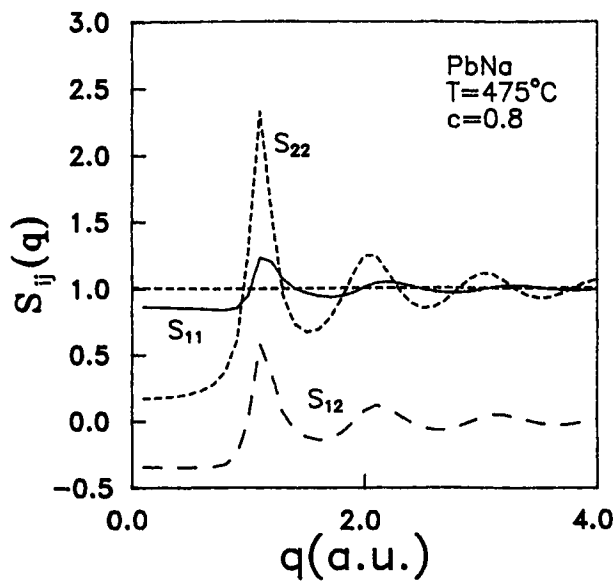| Metal	n	σ	A_0	A_1	A_2	R_M
Li	0.00841	4.709	0.336	0.504	0.455	2.800
Na	0.00359	6.253	0.305	0.339	0.402	3.400
K	0.00187	7.781	0.240	0.256	0.368	4.200
Pb	0.00459	5.764	1.920	2.000	0.900	2.100

T. KHAJIL

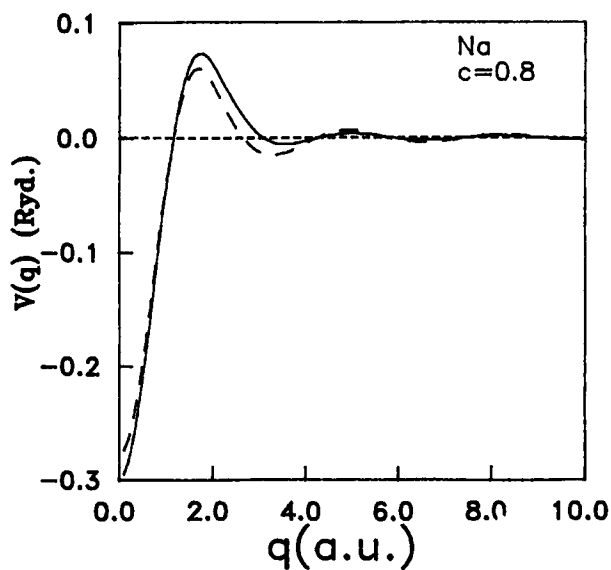
FIGURE 1   Partial structure factors for Pb–Na.

FIGURE 2a   Heine-Abarenkov model potential for Na. Solid line denotes nonlocal potential and dashed line denotes local one.
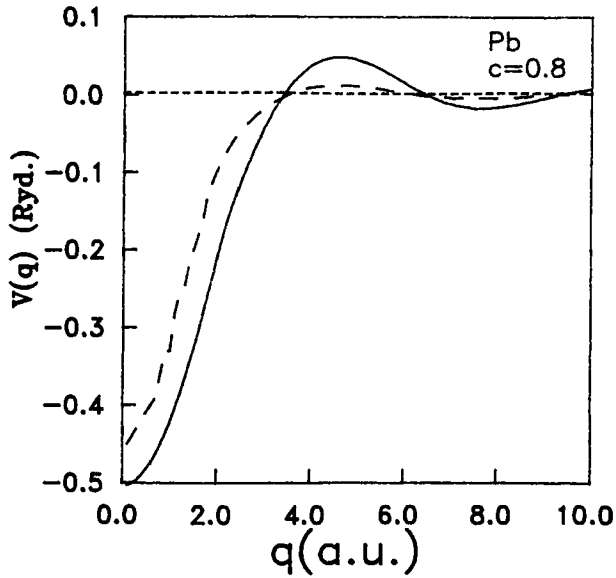
FIGURE 2b   Heine-Abarenkov model potential for Pb. Solid line denotes nonlocal potential and dashed line denotes local one.
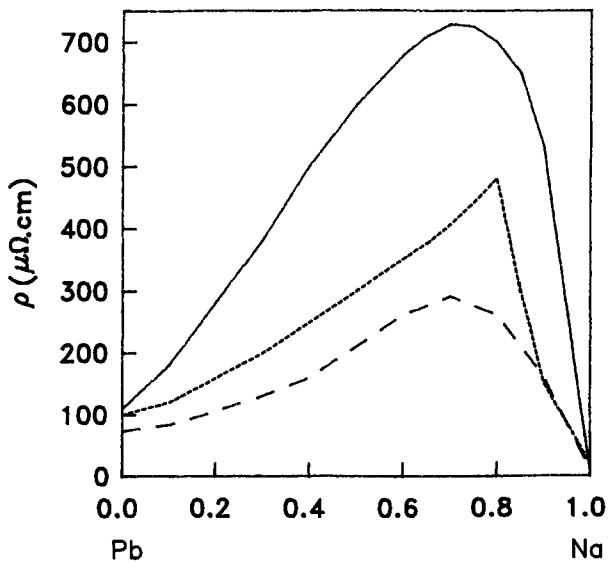

FIGURE 3   The resistivity values for liquid Pb–Na. Solid line denotes AM resistivity, dashed line denotes FZ resistivity and dotted line denotes experimental values.
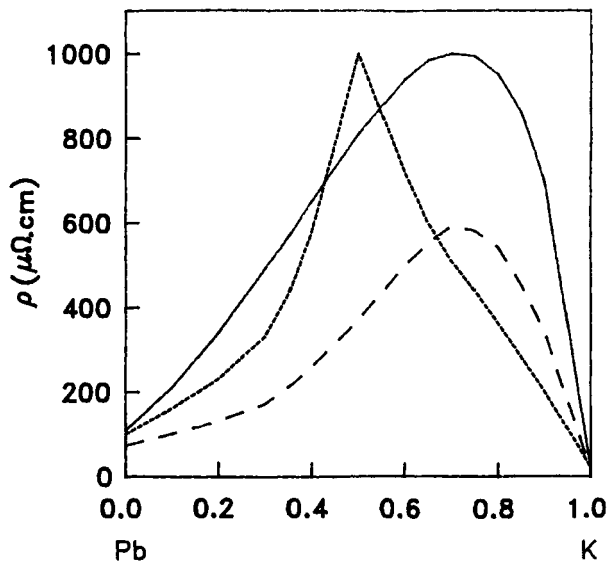
FIGURE 4   The resistivity values for liquid Pb–K. Solid line denotes AM resistivity, dashed line denotes FZ resistivity and dotted line denotes experimental values.
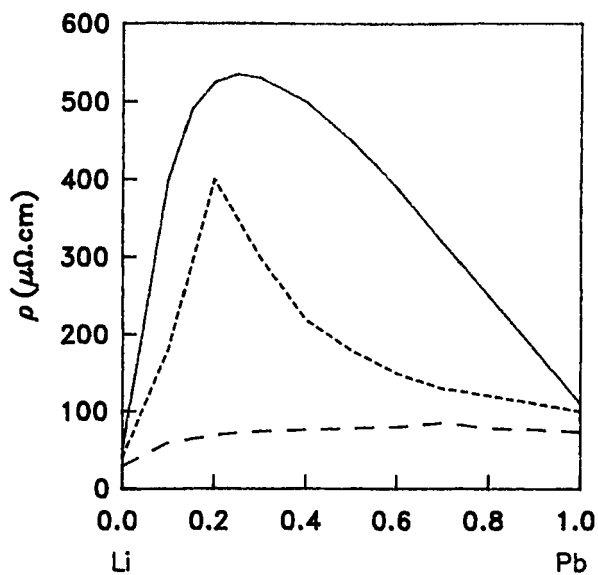
FIGURE 5   The resistivity values for liquid Li–Pb. Solid line denotes IS resistivity, dashed line denotes FZ resistivity and dotted line denotes experimental values.

In any case, the results establish that the modified finite mean free path effect and the nonlocal potentials alter significantly the calculated resistivity values for these alloys from that given by Ziman formula as discussed by [6].

We add here two other points:

1. Since the resistivity values are most sensitive to the pseudopotential parameters employed in these calculations they have been kept constant throughout the concentration range.
2. The calculated resistivity values for each liquid alloy considered here have been found to be such that $\rho_{AM} > \rho_{FZ}$. This is in agreement with other calculations [6].

In addition, the full mean free path dependent screening function is employed in this work.

To conclude, we observe that the inclusion of the mean free path effects in the screening function considerably improves the results. Furthermore we see that the Ascough-March formula with nonlocal potentials yields better agreement with observed resistivity values, because it includes in a self-consistent manner the mean free path for electron-ion scattering into the formalism of electron transport based on the force–force correlation approach.

References

[1] Meijer, J. A., Greetsma, W. and Van der Lugt, W. (1985). *J. Phys. F*, **15**, 899.
[2] Xu, R., de Jonge, T. and Van der Lugt, W. (1993). *J. Non-crys. Solids*, **156**, 293.
[3] Van der marel, Van Oosten, A. B., Geertsma, W. and Van der Lugt, W. (1982). *J. Phys. F*, **12**, 2349.
[4] Faber, T. E. and Ziman, J. M. (1967). *Philos. Mag.*, **11**, 153.
[5] Ferraz, A. and March, N. H. (1979). *Phys. Chem. Liq.*, **8**, 271.
[6] Leavens, C. R., Macdonald, A. H., Taylor, R., Ferraz, A. and March, N. H. (1981). *Phys. Chem. Liq.*, **11**, 115.
[7] Khajil, T. M. A. and Tomak, M. (1986). *Phys. Stat. Sol. (b)*, **134**, 321.
[8] Daver, F., Khajil, T. M. A. and Tomak, M. (1986). *Phys. Stat. Sol. (b)*, **138**, 373.
[9] Ascough, J. A. and March, N. H. (1991). *Phys. Chem. Liq.*, **23**, 37.
[10] Ichimaru, S. and Utsomi, K. (1981). *Phys. Rev. B*, **21**, 7385.
[11] Abarenkov, I. V. and Heine, V. (1963). *Philos. Mag.*, **12**, 528.
[12] Animalu, A. O. E. (1965a). *Philos. Mag.*, **11**, 379.
[13] Heine, V. and Abarenkov, I. V. (1964). *Philos. Mag.*, **9**, 451.
[14] Animalu, A. O. E. and Heine, V. (1965). *Philos. Mag.*, **12**, 1249.
[15] Animalu, A. O. E. (1973). *Phys. Rev. B*, **8**, 3542.
[16] Ashcroft, N. W. and Langreth, D. C. (1967). *Phys. Rev.*, **159**, 500.
[17] Waseda, Y., *The Structure of Non-Crystalline Materials* (1980, MacGraw Hill Iut Books Company).

[18] Koubaa, N. and Gasser, J. G. (1990). *J. Non-Crys. Solids*, **117/118**, 308.
[19] Koubaa, N., Anno, L. and Gasser, J. G. (1990). *J. Non-Crys. Solids*, **117/118**, 312.
[20] Koubaa, N. and Gasser, J. G. (1990). *J. Non-Crys. Solids*, **117/118**, 316.